

MgO Nanoparticles for the Removal of Reactive dyes from Wastewater

N. Jamil*, M. Mehmood*, A. Lateef*, R. Nazir** and N. Ahsan***

*College of Earth and Environmental Sciences, University of the Punjab, Lahore, Pakistan

**Pakistan Council for Scientific and Industrial Research, Lahore, Pakistan

***Institute of Geology, University of the Punjab, Lahore, Pakistan

ABSTRACT

Decolorization of textile wastewater is a significant environmental issue. In present study magnesium oxide nanoparticles with crystalline size of 19 nm were successfully synthesized by co-precipitation method and characterized through FT-IR and XRD techniques. The adsorption behavior of MgO nanoparticles was evaluated in batch set up for the removal of Reactive Black 5 and Reactive Orange 122 from synthetic dye solution. The adsorption equilibrium attained at contact time of 50 and 70 minutes, adsorbent dose 0.025g and 0.03g and pH 10 and 2 for Reactive Black 5 and Reactive Orange 122 respectively. While shaking speed was 150 rpm and initial dye concentration of 100 mg/L for both dyes. The adsorption data well fitted to Langmuir and Freundlich isotherms indicating the feasibility of adsorption process. Adsorption capacities q_{max} , 500 and 333.34 mg/g for Reactive black 5 and Reactive Orange 122 respectively. Thermodynamic parameters were evaluated for the adsorption data.

Keywords: MgO, nanoparticle, adsorption, RB5, RO122

1 INTRODUCTION

All over the world contamination of water resources is mainly due to increase in urbanization and industrialization [1]. Among these pollutants, significant quantities of synthetic dyes contribute a lot in water pollution [2]. In textile industry wet processes like bleaching, printing and dyeing consume large volumes of water along with various chemicals in textile industry. Unfixed dyes from rinsing operation and spent dye bath, both make wastewater exceedingly colored [3]. Nearly 20-50 % of dyes remains unfixed and is discharged into wastewater [4]. These dyes negatively affect the aesthetical value of water bodies and cause annoyance to the aquatic life by affecting penetration of sunlight which ultimately reduces the photosynthetic activity and inhibit the development of aquatic flora and fauna [5]. Approximately one million tons of these dyes are manufactured per annum around the world [6].

Nanotechnology is an emerging technology of 21st century. These nanoparticles present considerable advances in wastewater treatment with their significantly high surface area along with their sorption sites, specific pore size, small

intraparticle distance and their surface chemistry. In present study, Reactive Black 5 (RB5) and Reactive Orange 122 (RO122) were selected to analyze the behavior of adsorption. RB5 and RO122 both are azo dyes, with molecular formula $C_{26}H_{21}N_5Na_4O_{19}S_6$ and $C_{31}H_{20}ClN_7Na_4O_{16}S_5$ respectively. Massive amounts of reactive azo dyes are consumed in textile sector for cotton and wool dyeing due to their cost and color variety but the main problem associated with their usage is their fixing ability to the fabric. Nearly 50% of these dyes remain unfixed due to inefficiency in industrial processing [7].

2 EXPERIMENTAL

2.1 Synthesis of Adsorbent

Co-precipitation method was adopted for the synthesis of MgO nanoparticles [8]. 10.165g of hydrated magnesium chloride ($MgCl_2 \cdot 6H_2O$) was dissolved in doubly distilled deionized water and 500ml of 0.2 M solution of NaOH was taken in separating funnel and added drop-wise into $MgCl_2$ solution with continuous stirring through magnetic stirrer. After dropping, the precipitates were filtered along with gentle washing. Then precipitates of MgO were dried in oven at $110^\circ C$ for 3-4 hours and then placed in muffle furnace at $600^\circ C$ for 3-4 hours. White colored powdered MgO nanoparticles were prepared.

2.2 Batch Study

Batch experiments were performed to evaluate the effect of different parameters on adsorption process. Known volumes of dye solutions were taken in conical flasks and measured amounts of the adsorbent were added into it. All the conditions were kept constant in the each experiment except for the one which was under examination.

3 RESULTS AND DISCUSSION

3.1 FTIR Analysis

MgO nanoparticles were characterized by FTIR spectroscopy. The spectra were measured over the range of $400-4000\text{ cm}^{-1}$ (Fig.1 and Fig. 2). The sharp peak at 3628.10 cm^{-1} is attributed to the OH antisymmetric stretching vibration in $Mg(OH)_2$. The peaks at 698.23 cm^{-1} and

788.89 cm^{-1} are assigned to the Mg–O stretching vibration. The absorption peaks at 1483.26 cm^{-1} and 1598, 1010.70 cm^{-1} corresponds to the bending vibration of OH bond and Mg–OH stretching vibrations respectively. The other absorption peaks at 1687.71 cm^{-1} and 1872.88 cm^{-1} are due to the stretching and the bending vibration of water, respectively [9]. It has been observed from FTIR spectra of dye loaded MgO nanoparticles (Fig.2) that there is only slight change in one peak at 1155.36 cm^{-1} which might be due to some dye binding process on the surface of adsorbent.

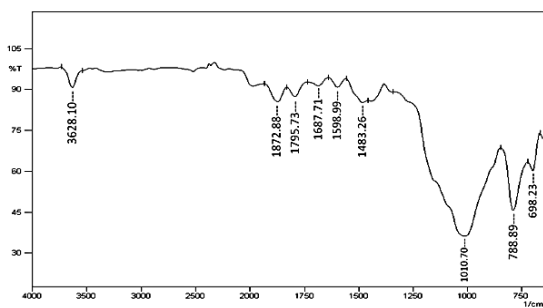


Fig.1: FTIR spectra of MgO Nanoparticles

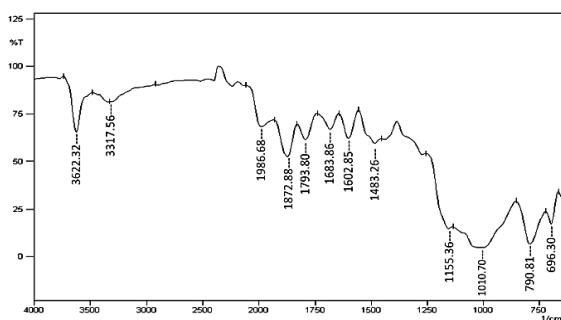


Fig. 2: FTIR Spectra of MgO nanoparticles after adsorption

3.2 XRD Analysis

MgO nanoparticles were analyzed through X-ray diffraction technique to study their crystalline nature. The results of crystallographic parameters showed cubic crystalline structure of MgO nanoparticles with crystalline size of 19 nm and measured density of 4.21 g/cm^3 . Fig. 3 and Fig.4 showed XRD peak pattern of MgO nanoparticles and XRD reference pattern of MgO nanoparticles respectively. XRD pattern of MgO nanoparticles was taken at position 2θ ranging from 10° – 80° . The resultant pattern showed five characteristic peaks at 2θ value were located at 36.932° , 42.906° , 62.294° , 74.675° and 78.614° corresponding to 111, 200, 220, 311 and 222 crystal planes indicating the formation of cubic structure of Mg-O. The XRD data revealed that the synthesized MgO nanoparticles are similar to the cubic structure with the space group (Fm-3m) [10, 8].

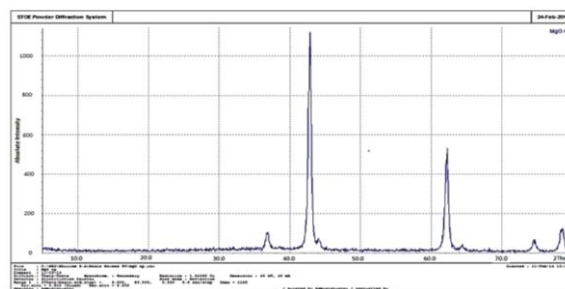


Fig.3: XRD peak pattern of MgO nanoparticles

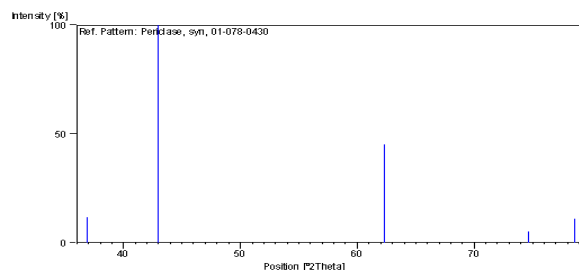


Fig.4: XRD Reference pattern of MgO nanoparticles

3.3 Effect of Shaking Speed

The effect of shaking for both dyes was studied and shown in Fig.5. The optimum removal efficiency was observed at 150 rpm for both metals with 93.91 % and 98.5% removal of RB5 and RO122 respectively. Other operational parameter were 0.02g adsorbent dose, 100 mg/L dye concentration, pH 7 and contact time 60min at 30 $^\circ\text{C}$. Fig.5 shows that adsorption first increases by increasing the shaking speed up to the optimum level and then it decreases. This behavior can be supported by the fact that after optimum limit further increase in speed results in breakdown of weak adsorption bonds [11].

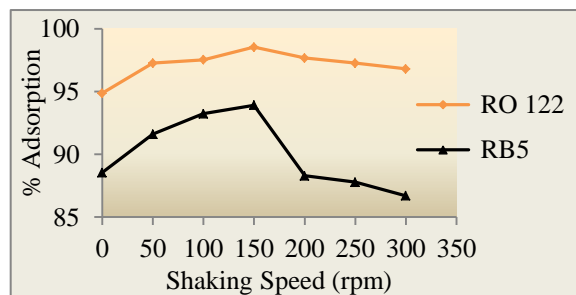


Fig.5: Effect of Shaking Speed on the adsorption of RB5 and RO122

3.4 Effect of Contact Time

To find out optimum time for maximum adsorption of both dyes on MgO nanoparticles, time varied from 10-120 minutes. Other parameters were kept constant like shaking speed 150 rpm, adsorbent dose 0.02g, initial dye

concentration 100 mg/L, pH 7 and temperature 30 °C. Fig.6 revealed that maximum adsorption occurs at 50 minutes for RB5 and 70 minutes for RO122. The resulted pattern may be justified that initially all the binding sites are readily available to dye molecules, so they can easily adhere. As the time increases, more and more sites of adsorbent become occupied until it reaches to optimum value and no further significant increase in adsorption occurs [12].

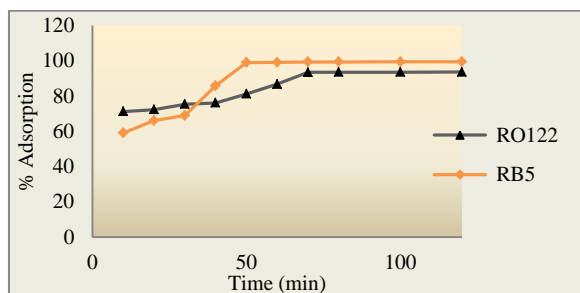


Fig.6: Effect of Time on the adsorption of RB5 and RO122

3.5 Effect of Adsorbent Dose

The effect of adsorbent dose was studied by varying the amount of adsorbent from 0.01-0.05g/L. All other operational parameters were kept constant; 150 rpm shaking speed, optimum time of both dyes, 100 mg/L initial dye concentration, pH 7 and 30 °C temperature. RB5 shows 99.26% adsorption at 0.025g while RO122 shows 99.53% removal at 0.03g (Fig.7). Increase in the removal efficiency of the dye is because of the presence of large amount of the binding sites for adsorption at higher adsorbent dose [13].

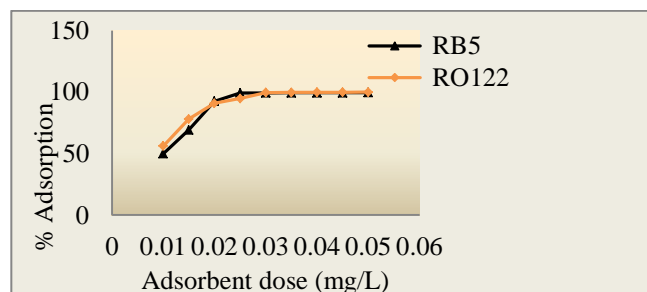


Fig.7: Effect of adsorbent dose on the adsorption of RB5 and RO122

3.6 Effect of pH

Effect of pH was studied by conducting experiments over a range of 2-12 pH. Optimized values of shaking speed, time and adsorbent dose were set at 30°C with initial dye concentration 100 mg/L. Fig.8 shows maximum removal at pH 10 for RB5 and pH 2 for RO122. At acidic and basic pH values the surface of the MgO nanoparticles would be surrounded by H⁺ and OH⁻ hydrogen and hydroxyl ions. These charged ions compete with the dye molecules and as the result of which adsorption decreases.

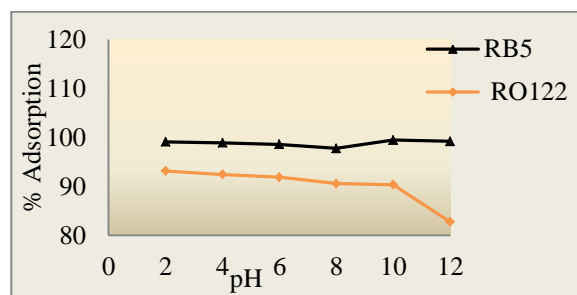


Fig.8: Effect of pH on the adsorption of RB5 and RO122

3.7 Effect of Temperature

To optimize temperature, experiments were executed at 10 to 70 °C temperature with other optimum conditions for both dyes. For RB5 maximum adsorption occurs at 50 °C while in case of RO122 is 70 °C (Fig. 9). This trend may be attributed as the adsorption of dyes increases with increase in temperature because the reaction energy increases which increases the adsorption capacity.

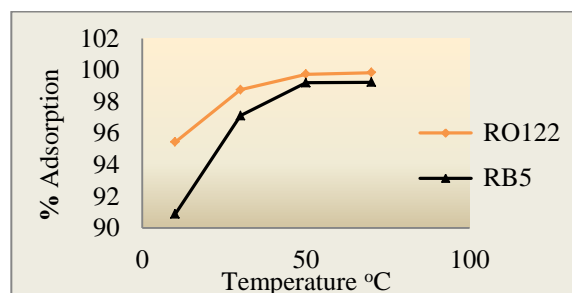


Fig.9: Effect of Temperature on the adsorption of RB5 and RO122

3.8 Langmuir Isotherm

Adsorption behavior was analyzed as a function of dye concentration at all optimum conditions, and the resultant data was utilized to evaluate Langmuir isotherm model. A straight line was attained by plotting a graph between 1/ C_e and 1/q for both dyes (Fig.10 and Fig. 11).

	Langmuir Constant			Freundlich Constant		
	q _{max} mg/g	b Lm/g	R ²	K _f mg/g	n	R ²
RB5	500	0.1	0.997	45.1	1.19	0.999
RO 122	333.3	0.3	0.973	73.7	1.73	0.992

Table 1: Langmuir and Freundlich Constants

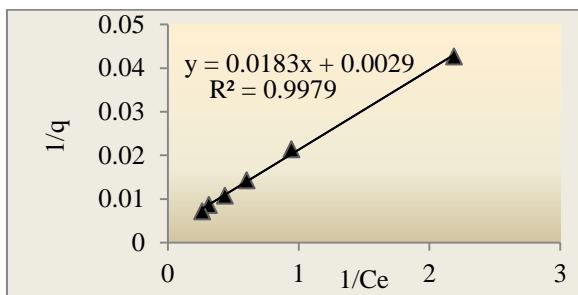


Fig.10: Langmuir Isotherm for RB 5

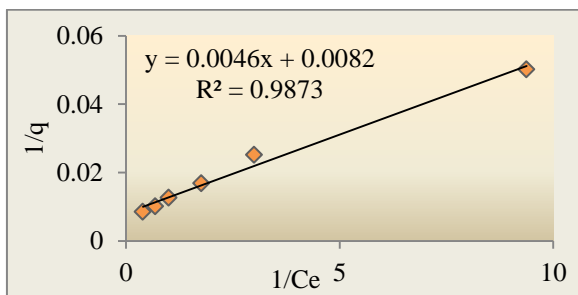


Fig.11: Langmuir Isotherm for RO122

3.9 Freundlich Isotherm

The adsorption data was evaluated through Freundlich model to study the adsorption behavior of RB5 and RO122 on MgO nanoparticles. Freundlich isotherm was plotted between $\log C_e$ and $\log q$ which results in straight lines (Fig.12 and Fig.13). Freundlich constants ' K_f ' and ' n ' were calculated and given in Table 1.

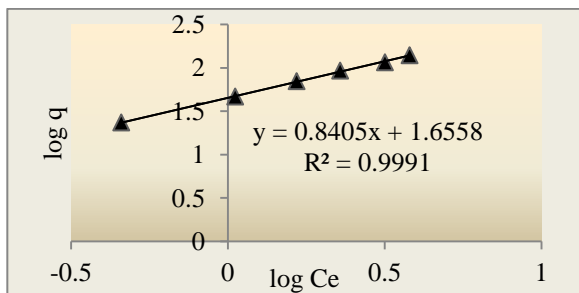


Fig.12: Freundlich Isotherm for RB5

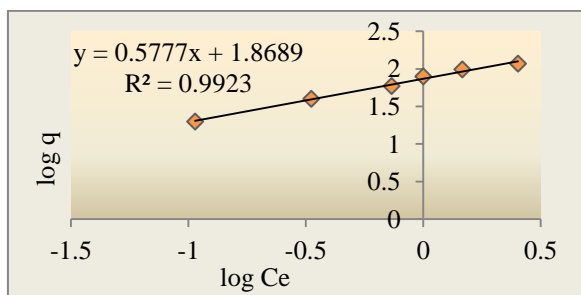


Fig.13: Freundlich Isotherm for RO122

3.10 Thermodynamic Parameters

Thermodynamic parameters were calculated from the experimental data of both dyes over a range of 293-303 K with all other parameters set at optimum conditions. Three different parameters i.e. Gibbs free energy, enthalpy and entropy change were calculated by plotting graph between inverse of T and $\ln K$ (Fig.14).

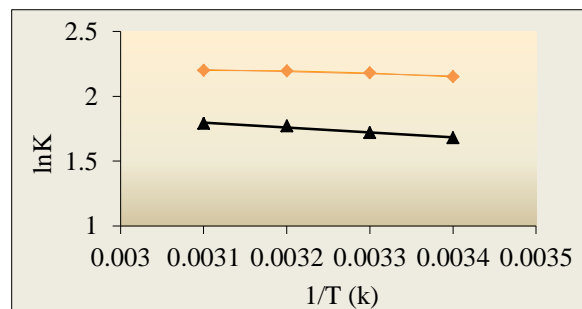


Fig. 14: $\ln K$ vs $1/T$

	ΔS° $\text{kJmol}^{-1}\text{K}^{-1}$	ΔH° kJmol^{-1}	ΔG kJmol^{-1}	R^2
RB 5	0.429	3.337	-1.905	0.970
RO 122	0.838	3.209	-2.155	0.983

Table.2: Thermodynamic Parameters

REFERENCES

- [1] M. Saeed, R. Nadeem and M. Yousaf, *Int J Environ Sci Te.*12, 1223, 2015.
- [2] A. Patil and J. Jadhav, *Chemosphere.* 92, 225, 2013.
- [3] A. R. T. Baga, N. M. Mahmoodi and F. M. Menger, *Desalination.* 260, 34, 2010.
- [4] A. Khalid, B. Saba, H. Kanwal, A. Nazir and M. Arshad, *Int Biodeter Biodegr.* 85, 550, 2013.
- [5] M. Asghar and H. N. Bhatti, *Ecol Eng.* 36, 1660, 2010.
- [6] S.A.S.Chatta, M. Asgher, S. Ali and A. I. Hussain, *Carbohydr Polym.* 87, 1476, 2012.
- [7] R. Bibi, M. Arshad and H. N. Asghar, *Int J Agri & Bio.* 14, 353, 2012.
- [8] T. G. Venkatesha, Y.A. Nayaka and B.K. Chethana, *Appl Surf Sci.* 276, 620, 2013.
- [9] R. Kumar, A. Sharma and N. Kishore, *Int J Eng App & Manag Sc Parad.* 07, 16, 2013.
- [10] A. V. Borhade, K. G. Kanade, D. R. Tope, and M.D. Patil, *Res Chem Intermediat.* 38, 1931, 2012.
- [11] T. Madrakian, A. Afkhami, H. M. Kashani and M. Ahmadi, *J Iran Chem Soc.* 10, 481, 2013.
- [12] N. K. Nga, P. T. T. Hong, T. D. Lam and T. Q. Huy, *J Colloid Interf Sci.* 398, 210, 2013.
- [13] E. Erdem, G. Colgecen and R. Donat, *J Colloid Interf Sci.* 282, 314, 2005.